

$^{31}\text{P}\{^{27}\text{Al}\}$ MQMAS/HETCOR NMR Study on Structure of Amorphous AlPO_4 Takahiro Iijima,* Koji Kanehashi,[†] Koji Saito,[†] Moriaki Hatakeyama,[†] Takahiro Nemoto,^{††}
Tadashi Shimizu, and Shinobu Ohki

National Institute for Materials Science, Tsukuba, Ibaraki 305-0003

[†]Nippon Steel Corporation, Futtsu, Chiba 293-8511^{††}JEOL Ltd., Musashino, Akishima, Tokyo 196-8558

(Received May 30, 2005; CL-050697)

A solid-state NMR method combining ^{27}Al multiple-quantum magic-angle spinning (MQMAS) and $^{31}\text{P}\{^{27}\text{Al}\}$ heteronuclear correlation (HETCOR) has been applied for the structural analysis of amorphous AlPO_4 . We obtained a correlation between the isotropic chemical shifts of ^{31}P in PO_4 and of ^{27}Al in each AlO_n ($n = 4, 5,$ and 6) distributed by the amorphous structure.

High-resolution solid-state NMR is an indispensable tool for analyzing the local structure of both inorganic and organic materials. Double rotation (DOR)¹ and dynamic angle spinning (DAS)² techniques can provide high-resolution NMR spectra of half-integer quadrupole nuclei, but require dedicated probe hardware that controls two sample rotations in order to average the second-order quadrupole interaction. In 1995, Frydman and co-workers developed another method called as multiple-quantum magic-angle spinning (MQMAS) for obtaining the high-resolution spectrum of the quadrupole nuclei.³ The MQMAS method that can use the conventional MAS probe has been widely used for the structural analysis of materials such as zeolites, glasses, and minerals.⁴ Recently, MQMAS has been extended to acquire a heteronuclear correlation in the presence of the quadrupole nuclei (MQMAS/HETCOR).⁵ Although MQMAS/HETCOR allows us to obtain easily the correlation from the spectrum expanded into two dimensions, few applications of this method for the structural characterization of the materials have been reported so far.

Solid-state NMR is capable of characterizing the structure of amorphous materials that is difficult by using diffraction methods. Both of crystalline and amorphous materials exist for aluminum phosphate (AlPO_4).^{6–8} Although the structure of AlPO_4 composed of PO_4 and AlO_n ($n = 4, 5,$ and 6) polyhedron has been completely determined for some of crystalline sample,^{6,7} only little is known for amorphous one ($\alpha\text{-AlPO}_4$). Kraus and co-workers have estimated the values of quadrupole coupling constant and isotropic chemical shift of ^{27}Al ($S = 5/2$) in $\alpha\text{-AlPO}_4$ by measuring the ^{27}Al MQMAS spectrum.⁸ The ^{27}Al isotropic chemical shift was found to distribute largely by the amorphous structure. Previously, we investigated the local structure at ^{17}O and ^{31}P ($I = 1/2$) sites of $\alpha\text{-AlPO}_4$ by measuring $^{17}\text{O} \leftrightarrow ^{31}\text{P}$ mutual cross polarization (CP) and ^{17}O MQMAS.⁹ In the present work, we apply the MQMAS/HETCOR method for the structural analysis of $\alpha\text{-AlPO}_4$. The distribution of P–O–Al bond angle of neighboring polyhedron of AlO_n and PO_4 is discussed from the $^{31}\text{P}\{^{27}\text{Al}\}$ MQMAS/HETCOR spectrum.

Figure 1 shows the pulse sequence of MQMAS/HETCOR used in this work. We briefly mention this sequence that consists of ^{27}Al z-filtering (ZF) MQMAS¹⁰ and $^{27}\text{Al} \rightarrow ^{31}\text{P}$ CPMAS. The

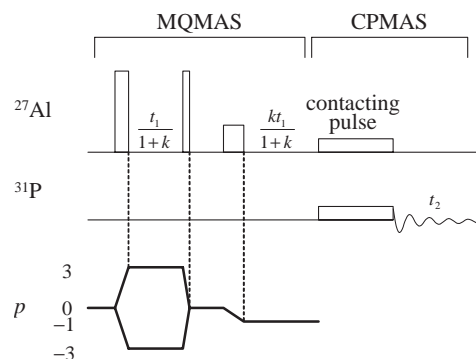


Figure 1. Pulse sequence and coherence pathway of the $^{31}\text{P}\{^{27}\text{Al}\}$ MQMAS/HETCOR experiment. p represents the order of coherence for ^{27}Al . k is equal to $19/12$ for spin- $5/2$ nuclei.

first and second hard pulses in ZF-MQMAS excite the triple-quantum coherence of ^{27}Al and convert from triple- to zero-quantum coherence, respectively. After the ZF delay, the soft reading pulse is irradiated to generate the single-quantum coherence. The evolution time t_1 is split into two regions, (i) evolution under triple-quantum coherence with duration $t_1/(1+k)$ and (ii) evolution under single-quantum coherence with $kt_1/(1+k)$, where k is equal to $19/12$ for ^{27}Al . This makes it possible for an isotropic echo³ to appear always at the end of t_1 . The ^{27}Al magnetization due to the isotropic echo is transferred to ^{31}P using the $^{31}\text{P}\text{-}^{27}\text{Al}$ dipolar interaction by the contacting pulse. Finally, the ^{31}P signal is acquired during t_2 . Double Fourier transform provides the high-resolution $^{31}\text{P}\{^{27}\text{Al}\}$ HETCOR spectrum.

The $\alpha\text{-AlPO}_4$ material used was the same sample as studied in ref 9. The $^{31}\text{P}\{^{27}\text{Al}\}$ MQMAS/HETCOR spectrum was recorded at 16.4 T on a JEOL ECA 700 spectrometer. We used a JEOL XY 4 mm MAS probe employing a balanced resonator type electric circuit, which enables us to irradiate the hard pulses. The resonant frequencies of ^{31}P and ^{27}Al were 283.416 and 182.430 MHz, respectively. The MAS frequency of $\nu_r = 18$ kHz was stabilized within ± 10 Hz by a JEOL MAS speed controller. The ^{31}P and ^{27}Al chemical shifts were referenced to 85% H_3PO_4 solution at 0 ppm and 1.0 M AlCl_3 solution at -0.1 ppm, respectively.

Figure 2a shows the $^{31}\text{P}\{^{27}\text{Al}\}$ MQMAS/HETCOR spectrum of the powder sample of $\alpha\text{-AlPO}_4$. F_1 and F_2 axes represent the chemical shifts of ^{27}Al and ^{31}P , respectively. The MQMAS/HETCOR spectrum using the sequence in which both of the echo ($0 \rightarrow +3 \rightarrow 0 \rightarrow -1$) and antiecho ($0 \rightarrow -3 \rightarrow 0 \rightarrow -1$) pathways are included in the MQMAS block exhibits ghost peaks due to the latter pathway.¹³ Such a peak exists about at

90–130 ppm in F_1 dimension of Figure 2a. The projection of the MQMAS/HETCOR spectrum onto the F_2 axis corresponds to the conventional ^{31}P MAS NMR spectrum, while that onto the F_1 axis represents the ^{27}Al high-resolution spectrum free from the broadening due to the second-order quadrupole coupling. The peaks at ca. 0, 27, and 48 ppm of F_1 -projected spectrum can be attributed to the ^{27}Al in AlO_6 , AlO_5 , and AlO_4 , respectively, by their peak positions.⁸ The remaining broadening in F_1 -projected spectrum is due to the distribution of the ^{27}Al isotropic chemical shift caused by the amorphous structure, because the distribution of the quadrupole coupling constant is quite small in a- AlPO_4 .⁸ Therefore, the $^{31}\text{P}\{^{27}\text{Al}\}$ MQMAS/HETCOR spectrum of a- AlPO_4 represents the correlation of the isotropic chemical shift for ^{31}P in PO_4 tetrahedron and ^{27}Al in each AlO_n polyhedron. We note that the broadening due to the dipolar interaction of the heteronuclear spins in the spectra of ^{31}P and ^{27}Al dimensions can be really removed by MAS. Assuming P–O distance of 0.152 nm, O–Al distance of 0.173 nm⁷ and P–O–Al angle of $140 \pm 10^\circ$ and considering the four nearest ^{17}O – ^{27}Al spins for ^{31}P NMR and six nearest ^{17}O – ^{31}P spins for ^{27}Al NMR, the linewidth of the ^{31}P and ^{27}Al spectra were calculated as 4.2 ± 0.8 and 1.5 ± 0.3 kHz, respectively, from the second moment analysis.¹⁴ These values are considerably smaller than the MAS frequency of $\nu_r = 18$ kHz.

In order to discuss the structure of a- AlPO_4 , we sliced the ^{31}P spectrum at the F_1 frequency of 0 ppm (AlO_6), 27 ppm (AlO_5), and 48 ppm (AlO_4), as shown in Figure 2b. The ^{31}P sliced spectra for AlO_6 , AlO_5 , and AlO_4 were fitted by 1, 2 and 1 Gaussian lines, respectively. The central frequency ν_c and full width at half-maximum $\nu_{1/2}$ were as follows: (ν_c , $\nu_{1/2}$) = (–23 ppm, 14 ppm) for AlO_6 , (–18 ppm, 12 ppm) and (–31 ppm, 9 ppm) for AlO_5 , and (–26 ppm, 14 ppm) for AlO_4 . Unfortunately, the quantitative analysis cannot be performed owing to the usage of both CP and MQ in our experiment. Although distribution of the local bonding parameters such as the

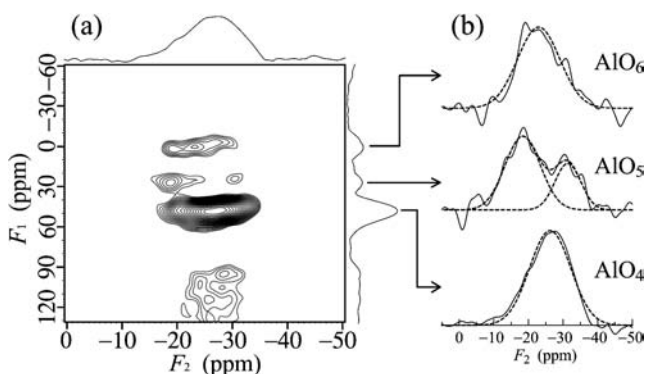


Figure 2. (a) $^{31}\text{P}\{^{27}\text{Al}\}$ MQMAS/HETCOR spectrum of a- AlPO_4 and projections along F_1 (aluminum) and F_2 (phosphorus) dimensions. The ^{27}Al irradiation frequency ν_1 and width p_w of first, second, and third pulses in the MQMAS block were (ν_1 , p_w) of (140 kHz, 3.0 μs), (140 kHz, 1.4 μs) and (13 kHz, 14 μs), respectively. The contacting pulses employed in the CPMAS block were $\nu_1(^{27}\text{Al}) = 8$ kHz and $\nu_1(^{31}\text{P}) = 4$ kHz which nearly fulfill the Hartmann–Hahn condition¹¹ modified for quadrupole spins under MAS,¹² $3\nu_1(^{27}\text{Al}) - \nu_r = \nu_1(^{31}\text{P})$. The CP contact time was 2.5 ms. (b) ^{31}P slice spectrum of (a) at the F_1 frequency of 0 ppm (AlO_6), 27 ppm (AlO_5), and 48 ppm (AlO_4). The broken line shows the Gaussian fitting.

bond angle, bond distance, and electron density can cause the broadening of the spectra, only the bond angle has been reported to correlate with the ^{31}P spectrum as far as we know.^{6,15} The ^{31}P spectrum of crystalline AlPO_4 shows a higher field shift with increasing mean bond angle ($\theta_{\text{P-O-Al}}$). For example, the ^{31}P chemical shift of –5.7, –20.6, and –24.5 ppm in AlPO_4 -14 corresponds to $\theta_{\text{P-O-Al}}$ of 130.4, 138.2 (or 139.7), and 144.1 $^\circ$, respectively. Furthermore, the ^{31}P – ^{27}Al correlation spectra by the through-bond J coupling and through-space dipolar coupling are almost the same as in AlPO_4 -14,⁶ and both of the correlations indicate the connectivity between neighboring polyhedron of PO_4 and AlO_n . In this work, we assume that the ^{31}P chemical shift and ^{31}P – ^{27}Al correlation in the amorphous sample are similarly assigned as in crystalline AlPO_4 -14; the chemical shift of the ^{31}P slice spectrum corresponds to $\theta_{\text{P-O-Al}}$ for the neighboring polyhedron of PO_4 and AlO_n . The simultaneous high-field shift of the spectrum for ^{31}P and ^{27}Al in AlO_4 (Figure 2a) supports our assumption, because the spectrum of ^{27}Al in AlO_4 has been also reported to shift to higher field with increasing $\theta_{\text{P-O-Al}}$.¹⁵ By comparing the ν_c and $\nu_{1/2}$ values, the distributions of $\theta_{\text{P-O-Al}}$ relevant to AlO_6 and AlO_4 are found to be different with respect to the central angle of the distribution. On the other hand, there exist two distinct distributions for $\theta_{\text{P-O-Al}}$ associated with AlO_5 . Therefore, we can conclude that the distribution function of $\theta_{\text{P-O-Al}}$ depends on the type of AlO_n polyhedron surrounding PO_4 tetrahedron.

In summary, the $^{31}\text{P}\{^{27}\text{Al}\}$ MQMAS/HETCOR spectrum has been measured for a- AlPO_4 and we obtained the connection between the isotropic chemical shifts of ^{31}P in PO_4 and of ^{27}Al in each AlO_n ($n = 4, 5$, and 6). It is suggested that the function of the distribution of $\theta_{\text{P-O-Al}}$ caused by the amorphous structure depends on the type of AlO_n bonding to PO_4 .

References

- 1 A. Samoson, E. Lippmaa, and A. Pines, *Mol. Phys.*, **65**, 1013 (1988).
- 2 A. Llor and J. Viret, *Chem. Phys. Lett.*, **152**, 248 (1988); K. T. Mueller, B. Q. Sun, G. C. Chingas, J. W. Zwanziger, T. Terao, and A. Pines, *J. Magn. Reson.*, **86**, 470 (1990).
- 3 L. Frydman and J. S. Harwood, *J. Am. Chem. Soc.*, **117**, 5367 (1995); A. L. Medek, J. S. Harwood, and L. Frydman, *J. Am. Chem. Soc.*, **117**, 12779 (1995).
- 4 C. A. Fyfe, J. L. Bretherton, and L. Y. Lam, *J. Am. Chem. Soc.*, **123**, 5285 (2001); J. F. Stebbins and Z. Xu, *Nature*, **390**, 60 (1997); L.-S. Du and J. F. Stebbins, *Chem. Mater.*, **15**, 3913 (2003).
- 5 S. H. Wang, S. M. De Paul, and L. M. Bull, *J. Magn. Reson.*, **125**, 364 (1997); S. Steuernagel, *Solid State Nucl. Magn. Reson.*, **11**, 197 (1998); G. Mali, J.-P. Amoureux, and V. Kaucic, *Phys. Chem. Chem. Phys.*, **2**, 5737 (2000).
- 6 C. A. Fyfe, H. M. zu Altenschildesche, K. C. Wong-Moon, H. Grondey, and J. M. Chezeau, *Solid State Nucl. Magn. Reson.*, **9**, 97 (1997).
- 7 H. K. Beyer and I. Belenykaya, *Stud. Surf. Sci. Catal.*, **5**, 203 (1980); J. J. Pluth and J. V. Smith, *Acta Crystallogr.*, **C42**, 283 (1986).
- 8 H. Kraus, R. Prins, and A. P. M. Kentgens, *J. Phys. Chem.*, **100**, 16336 (1996).
- 9 K. Kanehashi and K. Saito, *Chem. Lett.*, **2002**, 668.
- 10 J.-P. Amoureux, C. Fernandez, and S. Steuernagel, *J. Magn. Reson., Ser. A*, **123**, 116 (1996).
- 11 S. R. Hartmann and E. L. Hahn, *Phys. Rev.*, **128**, 2042 (1962).
- 12 A. J. Vega, *J. Magn. Reson.*, **96**, 50 (1992); A. J. Vega, *Solid State Nucl. Magn. Reson.*, **1**, 17 (1992).
- 13 C. Fernandez, C. Morais, and M. Pruski, *Phys. Chem. Chem. Phys.*, **3**, 2552 (2001).
- 14 A. Abragam, "Principles of Nuclear Magnetism," Oxford, London (1961); C. P. Slichter, "Principles of Magnetic Resonance," Springer-Verlag, New York (1990).
- 15 D. Muller, E. Jahn, G. Ludwig, and U. Haubenreisser, *Chem. Phys. Lett.*, **109**, 332 (1984).